

1 A Heterogeneous Visual Imaging Model for Analyzing the Impact of Vehicle Type on
2 Car-Following Dynamics

3
4 Liang Zheng, Ph.D. Candidate
5 Institute of Systems Engineering, College of Management & Economics,
6 Tianjin University, Tianjin, China, 300072
7 Phone: 86-022-27404446 Fax: 86-022-27404446
8 Email: zhengliang_tju@hotmail.com

9
10 Dr. Peter J. Jin, Postdoctoral Fellow
11 Department of Civil, Architectural, and Environmental Engineering,
12 University of Texas at Austin, Austin, TX 78701
13 Phone: 1-512-232-3124 Fax: 512-232-3153
14 Email: jjin@austin.utexas.edu

15
16 Dr. Yang Cheng, Research Associate
17 Department of Civil & Environmental Engineering,
18 University of Wisconsin-Madison,
19 Madison, WI 53706, USA
20 cheng8@wisc.edu

21
22 Dr. Shoufeng Ma, Professor
23 Institute of Systems Engineering, College of Management & Economics,
24 Tianjin University, Tianjin, China, 300072
25 Phone: 86-022-27404446 Fax: 86-022-27404446
26 Email: sfma@tju.edu.cn

27
28 Dr. Bin Ran, Ph.D., Professor
29 Department of Civil & Environmental Engineering
30 University of Wisconsin-Madison,
31 1415 Engineering Drive, Madison, WI 53706, USA
32 Phone: 1-608-262-0052 Fax: 1-608-262-5199
33 Email: bran@wisc.edu

34 and
35 School of Transportation, Southeast University
36 No.2 Si Pai Lou, Nanjing 210096, China

37
38
39
40

1
2
3
4
5
6
7
8
9
10
11
12
13
14
15
16
17
18
19
20
21
22
23
24
25
26
27
28
29
30
31
32
33
34
35
36
37
38
39
40

Corresponding Author: Liang Zheng

Submitted for Presentation and Publication
to the 92nd Transportation Research Board Meeting

Submission Date: August. 1, 2012

5216 Words+4 Tables+5 Figures =7466 Words

ABSTRACT

Heterogeneity is an essential characteristic in car-following behaviors, which can be defined as the differences between the car following behaviors of driver/vehicle combination under comparable conditions. This paper proposes a Visual Imaging Model (VIM) with relaxed assumption on a driver's perfect perception for 3-D traffic information and uniform reaction to vehicles with different sizes in most existing car following models. The proposed model can generate greater stimuli to the followers from the leading vehicles with larger back sizes (i.e. defined as vehicle width \times vehicle height) and short distance to the following vehicles, but less changes in stimuli for the distant leading vehicles under various back sizes. The US101 NGSIM data set containing vehicle type/size information is used to evaluate the proposed model at the levels of single trajectory pair and vehicle types. The calibration and validation results show the promising performance of the proposed model in describing heterogeneous car-following behavior. In this study, it is also found from US101 NGSIM data set that in relatively high velocity range, the following gap distance for car following truck (C-T) is greater than that for car following car (C-C), while in low velocity range, C-T has a smaller spacing than C-C. The phenomenon can also be reproduced by the proposed model.

1 INTRODUCTION

2 Heterogeneity is an essential characteristic in car following behaviors and can be defined as
3 the differences between the car following behaviors of driver/vehicle combination under
4 comparable conditions (1). The heterogeneous driving behavior studies usually include three
5 aspects of the general problem: different driving styles within a vehicle group of the same
6 vehicle type, different driving styles related to the different vehicle types, different driving
7 styles of the follower because of the leader's different vehicle type. Ossen and Hoogendoorn
8 (1) gained insights into the level of heterogeneity in car following behaviors in real traffic
9 under different types of heterogeneity. In another study (2), they pointed out the highly
10 different driving styles in car following behavior observed in a vehicle trajectory dataset
11 collected from a helicopter and also explored the feasibility of incorporating different types
12 and degree of heterogeneity in car following models. Ranjitkar et al.(3) investigated the
13 performance of some well-known microscopic traffic flow concepts based on different GPS
14 data and found that interpersonal variation are relatively higher than the intermodal variations.
15 Punzo and Tripodi (4) extend the single-class models to multiclass traffic scenario and
16 developed a calibration procedure for multiclass GIPPS car-following model. Meanwhile,
17 several researchers have concentrated on the following distance with respect to the vehicle
18 type. The following distance for car following truck (C-T) was found to be smaller than that
19 for car following car (C-C) in several different data sets (5,6,7). However, Yoo and Green (8)
20 obtained different conclusions that the following distance of C-C was 10% less than that C-T.
21 Ravishankar and Mathew (9) also concluded that the mean following distance varied across
22 vehicle-type combinations with smaller sized vehicles following at a closer spacing. The
23 contradicting results obtained by previous researchers about the following gap distances for
24 C-C and C-T indicate the necessity of studying the problem from a different viewpoint.

25 However, most existing car-following models were postulated for drivers' perfect
26 perception about 3-D traffic information (velocity, distance or acceleration) and homogenous
27 vehicle types. For example, the well-known General Motors (GM) model, firstly proposed by
28 Chandler et al. (10), utilizes the relative velocity between the leader and the follower as the
29 stimulus. Safe distance (SD) models pursue a safe following distance so as to avoid the
30 rear-end collision, one representative of which is Gipps' model (11). Optimal Velocity Model
31 (OVM) employs the difference between the current velocity and ideal velocity dependent on
32 the distance headway as the stimulus (12). Despite their success in describing the motion of

1 individual vehicles in continuous space and time from different aspects, there are some
2 deviations between the car-following behaviors described in those models and the reality. 1)
3 Car following behavior is a human decision-making and response process, and drivers can
4 not accurately perceive the 3-D traffic information, which violates the basic assumption of
5 those models. 2) Such car-following models do not have built-in mechanism to describe the
6 heterogeneous traffic flow composed of vehicles with different vehicle types. Multiple
7 sub-models with different model parameters need to be developed and calibrated to describe
8 each heterogeneous car-following scenario. However, it should be noted that Action Point
9 (AP) models set some perceptual thresholds of spacing or relative velocity to define the
10 minimum value of the stimulus to which the driver will react (13,14,15,16,17). Especially
11 drivers' perceiving the relative velocity between two successive vehicles is usually through
12 changes on the visual angle subtended by the vehicle in-front, which is definitely related to
13 the vehicle type/size of the preceding vehicle (15). Therefore, AP models can remedy above
14 two deviations in some degree.

15 Moreover, many other researchers have also considered different kinds of projected 2-D
16 visual information related to the vehicle type/size of the preceding vehicle when modeling the
17 car following behaviors, which can all be utilized to cope with the heterogeneous driving
18 behaviors due to the vehicle type/size. For example, Andersen and Sauer (18) presented
19 Driving by visual angel (DVA) model based on the framework of Helly's model (19), which
20 can produce more predictive driving performance than other models based on 3-D
21 information. Jin et al.(20) introduced a visual angle car following model by using the visual
22 angle and its change rate, which contributes to the design of more realistic car following
23 models. Lee and Jones (21) proposed a model that determines acceleration by the change rate
24 of the visual angle. On the other hand, Lee (22) showed that the inverse rate of expansion of
25 an approaching object (i.e. Denoted by τ) was a visual variable that could be used to estimate
26 the time to an impending collision, which was also investigated in the studies of driving
27 performance (23,24). However, when traffic flow is stable, τ usually keeps at an infinite
28 value. Therefore, it has limited usefulness in actual car following.

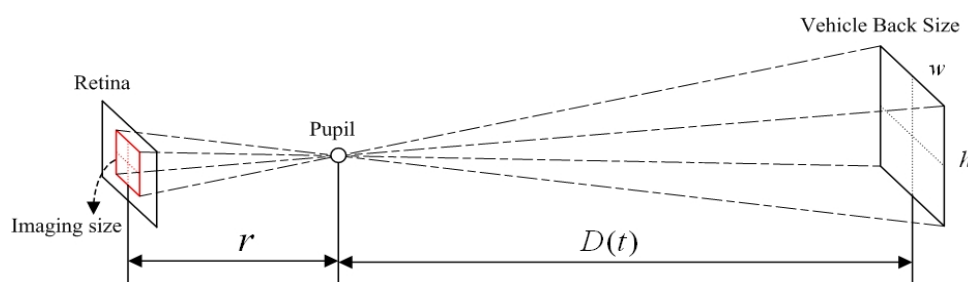
29 Besides, what worth our attention is that another candidate visual source is the visual
30 image information, which is related to two-dimensional information about the back size of
31 the leading vehicle. Michael (25) suggested that the image size of the preceding vehicle or its

1 visual extent could be used to model car following. Moreover, Zielke et al.(26) designed a
 2 computer algorithm for car following so as to maintain a constant image size of the preceding
 3 vehicle. Therefore, inspired by using the image information as the stimulus, in this paper, we
 4 utilize the visual imaging size of the leading vehicle and its change rate to replace the gap
 5 distance and relative velocity and propose the visual imaging model (abbreviated as VIM)
 6 based on the framework of Helly's model. The proposed VIM can not only relax the
 7 unrealistic assumption on a driver's perfect perception for the 3-D traffic information, but
 8 also can describe the heterogeneous driving behaviors caused by the various vehicle-type of
 9 the leader. The rest of the paper is organized as follows. First, VIM is proposed and analyzed.
 10 Then heterogeneous driving behaviors under different leader-follower compositions and
 11 velocity ranges are analyzed based on the US101 NGSIM data. After that, the rationality and
 12 performance of VIM in modeling the heterogeneous driving behaviors are evaluated. Finally,
 13 some important conclusions are drawn.

15 NEW VISUAL CAR FOLLOWING MODEL

16 The Proposed Visual Imaging Model

17 Existing vision based car-following models (15-21) usually approximate visual angles as the
 18 width of the leading vehicle divided by the gap distance, which only employs
 19 one-dimensional information of the leading vehicle (i.e. the vehicle width) and cannot
 20 effectively describe the stimulus to the follower from the back size of the leading vehicle.
 21 From the viewpoint of the visual imaging process, two-dimensional vehicle size information
 22 (i.e. the vehicle width and length) needs to be considered and incorporated into the modeling
 23 of the heterogeneous driving behaviors due to the leader's vehicle type.



24
25 **FIGURE 1 Illustration of the visual imaging**

26 According to the principle of visual imaging (cf. Figure 1), the back of the leading
 27 vehicle is projected on the retina of the following driver, therefore under the same gap

1 distance (denoted by $D(t)$) a leading vehicle with the larger back size will result in greater
 2 image size and cause stronger stimulus to the follower, which can be expressed as

$$3 \quad w/D(t) = w'/r \quad (1)$$

$$4 \quad h/D(t) = h'/r \quad (2)$$

$$5 \quad L_s/D(t)^2 = L_s'/r^2 \quad (3)$$

6 where w and h are the width and height of the leading vehicle respectively, w' and h' are the
 7 imaging width and height of the leading vehicle, r is the diameter of the eye, $L_s = w \cdot h$ is the
 8 back size of the leading vehicle, $L_s' = w' \cdot h'$ is the visual imaging size of the leading vehicle.

9 Moreover, Helly's model (19) can be served as the framework for VIM, which consists
 10 of a linear combination of a distance headway maintenance factor with a relative
 11 velocity-minimizing factor. The model ensures only when the desired distance headway has
 12 been achieved and the velocity difference is zero, the acceleration output is zero. After
 13 substituting the information of distance headway and relative velocity in Helly's model with
 14 appropriate factors related to visual information, similar stimuli in VIM come from two
 15 sources. One is the difference between the current and desired visual imaging size (i.e.
 16 maintenance factor). The other is the change rate of the visual imaging size (i.e. the
 17 minimizing factor). Besides, only when the desired visual imaging size has been reached, and
 18 the change rate of visual imaging size is zero, the acceleration output becomes zero.
 19 Therefore, the formulation of VIM can be expressed as

$$20 \quad a(t) = m \cdot [S_d(t) - S(t)] + n \cdot dS(t)/dt \quad (4)$$

21 where $S_d(t) = L_s \cdot r^2 / D_d(t)^2$ and $S(t) = L_s \cdot r^2 / D(t)^2$ indicate the desired and current visual
 22 imaging size of the leading vehicle respectively, $m > 0$ and $n < 0$ are the sensitivity
 23 coefficient, $D_d(t)$ is the desired gap distance between two successive vehicles and can be
 24 formulated as

$$25 \quad D_d(t) = \begin{cases} t_d \cdot v_f, v_f \geq v_j \\ s_0, v_f < v_j \end{cases} \quad (5)$$

26 where t_d is the desired time gap, v_f is the velocity of the following vehicle, s_0 is the gap
 27 distance in the traffic jam state, v_j is the critical velocity used to distinguish the traffic jam
 28 state. VIM model can then be rewritten as

$$29 \quad a(t) = m \cdot \left[\frac{r^2 \cdot L_s}{D_d(t)^2} - \frac{r^2 \cdot L_s}{D(t)^2} \right] + n \cdot \frac{d}{dt} \left[\frac{r^2 \cdot L_s}{D(t)^2} \right] \quad (6)$$

1 According to equation (6), the stimuli in VIM include two parts. One is the difference
 2 between the desired and current visual imaging size of the leading vehicle, which can be
 3 expressed as

$$c_d = \frac{r^2 \cdot L_S}{D_d(t)^2} - \frac{r^2 \cdot L_S}{D(t)^2} \tag{7}$$

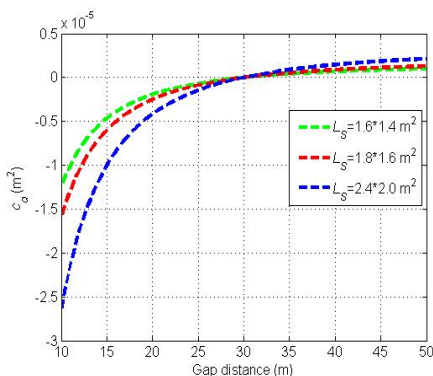
5 The other is the change rate of visual imaging size formulated as

$$c_r = \frac{d}{dt} \left[\frac{r^2 \cdot L_S}{D(t)^2} \right] = \frac{-2r^2 \cdot L_S \cdot \Delta V}{D(t)^3} \tag{8}$$

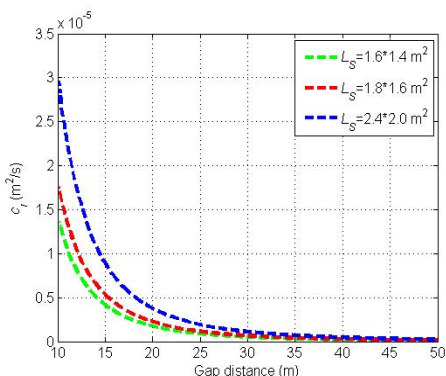
7 where the relative velocity $\Delta V = v_l(t) - v_f(t)$, $v_l(t)$ is the velocity of the leading vehicle.

8 **Performance Analysis of Visual Imaging Model**

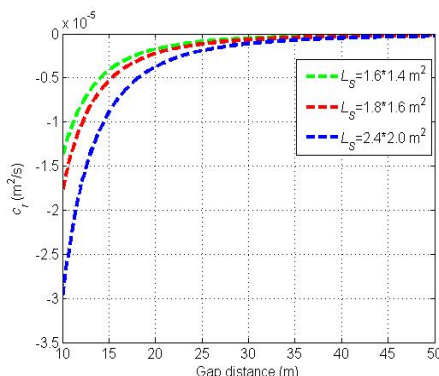
9 In order to understand the heterogeneous responses of the follower influenced by the leader's
 10 vehicle type, Figure 2(a) illustrates the relationship of the maintenance factor c_d and gap
 11 distance versus various L_S and Figure 2(b-c) shows the relationship between minimizing
 12 factor c_r and gap distance under different L_S .



(a)



(b)



(c)

1 **FIGURE 2 Relationship between driver response and the gap distance under different**
2 **L_S . $r=2.5*10^{-2}m$, (a) $t_d=2s$, $v_f=15m/s$, $v_r=3m/s$, (b) $\Delta V=-5m/s$, (c) $\Delta V=5m/s$**

3 In Figure 2(a) when the current gap distance $D(t)$ is smaller than the desired gap distance
4 $D_d(t)$ (30 m), the difference between the desired and current visual imaging size of the
5 leading vehicle (i.e. c_d) is negative, which means the follower has to decelerate to maintain
6 the desired visual imaging size. Meanwhile, under the same current gap distance the larger L_S
7 would result in greater absolute value of c_d . When $D(t)>D_d(t)$, c_d becomes positive, which
8 means the following vehicle need to accelerate to keep the desired visual imaging size, and
9 larger L_S results in greater c_d under the same gap distance. It should be noted that when
10 $D(t)\ll D_d(t)$, the difference of c_d under various L_S can be observed clearly because the driver
11 can easily identify back size of the leading vehicle. On the other, when $D(t)\gg D_d(t)$, such
12 difference is remarkably small because of the driver's difficulty in distinguishing the visual
13 imaging size of the leading vehicle.

14 In Figure 2(b), when $\Delta V < 0$ the following driver will brake to maintain the visual imaging
15 size, that is, to minimize the relative velocity with the preceding vehicle. Therefore, the value
16 of c_r is positive (Note: $n < 0$). Correspondingly in Figure 2(c), when $\Delta V > 0$ the follower needs to
17 accelerate and the value of c_r is negative. Meanwhile, Figure 2(b-c) also illustrates that under
18 the same gap distance, the absolute value of c_r is larger when the leading vehicle has larger
19 L_S . Meanwhile, compared with the situation of small gap distance, the value of c_r under
20 different L_S has insignificant change when $D(t)$ is relatively larger, which reflects that the
21 driver has difficulty in recognize the change of the visual imaging size when the leading
22 vehicle is extremely distant.

23
24 **VALIDATION OF THE HETEROGENEITY**

25 **Field Data Preprocessing**

26 It should be noted that there are some recording errors in the NGSIM data (27), e.g. the
27 values of acceleration or deceleration are unusually large, and the gap distance between two
28 successive vehicles is not larger than zero. Those errors should be removed before the further
29 selection of NGSIM data. Moreover, in order to detect the "close following" behaviors from
30 NGSIM data, the gap headway (in seconds) is used to describe the time gap from the rear of
31 the leading vehicle to the front of the following vehicle and the smaller time gap means the
32 closer car following behaviors. According to the characteristics of the NGSIM data, a value

of 3s for the gap headway (as also used by Sayer et al. (6) and Bennett (28)) has been chosen as the critical gap headway for “close following” behavior. Then the extracted vehicle trajectory data with the characteristic of “close following” can be further separated into different groups according to the leader-follower composition (e.g. C-C and C-T) and velocity range (e.g. $10 \leq V < 20$ (km/h), $20 \leq V < 30$ (km/h), $30 \leq V < 40$ (km/h), $40 \leq V < 50$ (km/h) and $50 \leq V < 60$ (km/h)). Note: the velocity range here is divided based on the averaged velocity of the following vehicle and each pair of leader-follower trajectories usually lasts for about 30 seconds. Finally, the averaged mean gap distance (MGD) can be calculated for each group. It should be noted that the gap distance is obtained based on NGSIM data by eliminating the vehicle length according to the composition of C-C or C-T.

Statistical Results

From the statistic results in table 1, it can be observed that the averaged MGDs for C-C are significantly different from those for C-T except within the velocity range of $20 \leq V < 30$ (km/h). For the velocity range $10 \leq V < 20$ (km/h), the averaged MGD for C-C is larger than that for C-T, which is the opposite for the averaged MGD of C-C and C-T within the velocity range of $30 \leq V < 40$, $40 \leq V < 50$ or $50 \leq V < 60$ (km/h). Furthermore, the unpaired *T*-test is used to check whether the averaged MGD for C-C in each velocity range is significantly different from that for C-T in the general case. That is, if $|t| > t_{0.05}(N_{C-C}-1+N_{C-T}-1)$, the averaged MGD for C-C is significantly different from that for C-T generally; otherwise, it is not significantly different from each other in the general case, where N_{C-C} and N_{C-T} are respectively the number of leader-follower trajectory pairs for C-C and C-T

TABLE 1 Statistic Results from Field Data US101

Velocity Range(km/h)	C-C		C-T		<i>T</i> -test	
	N_{C-C}	Averaged MGD (m)	N_{C-T}	Averaged MGD (m)	<i>T</i> values	<i>P</i> -values
[10,20)	284	8.7990	3	5.8734	$ t =2.2160$	$ t > t_{0.05}(285)$
[20,30)	722	12.2060	21	11.9774	$ t =0.2796$	$ t < t_{0.05}(741)$
[30,40)	1067	15.0525	38	16.3884	$ t =1.6533$	$ t > t_{0.05}(1103)$
[40,50)	453	17.3598	49	20.7709	$ t =4.0069$	$ t > t_{0.05}(500)$
[50,60)	29	20.7017	28	25.1970	$ t =2.0537$	$ t > t_{0.05}(55)$

From table 1, it is concluded that in the relatively low velocity range, e.g. $10 \leq V < 20$ (km/h), the averaged MGD for C-T is significantly smaller than that for C-C. However, in the relatively high velocity ranges, e.g. $30 \leq V < 40$, $40 \leq V < 50$ and $50 \leq V < 60$ (km/h), the averaged MGDs for C-T become significantly larger than those for C-C. Meanwhile, it should be noted that when the velocity range is $20 \leq V < 30$ (km/h), the averaged MGD for C-C is not significantly different from that for C-T. Therefore, it is easily known that in the relatively high velocity range, the follower is willing to keep a larger gap distance with the preceding truck to allow sufficient visual clearance for safe driving, which is completely different from that situation in the low velocity range. The cause can be analyzed empirically as follows: the leading truck with the higher velocity will produce more safety concerns to the follower than the leading car, which is because of the driver's different visual perception to the stimulus of the moving back size of the leading truck in various velocities.

VISUAL IMAGING MDOEL EVALUATION WITH NGSIM DATA

Evaluation Method

The averaged MGD for each group of vehicle trajectories can be utilized to determine the rationality of VIM in reproducing the heterogeneous driving behaviors. Meanwhile, for each pair of vehicle trajectories, Mean Absolute Relative Error (i.e. MARE) and Mean Absolute Error (MAE) are used to measure the difference between actual and simulated results during calibration, which take the following forms.

$$MARE = \frac{\sum_{t=1}^T |h^{sim}(t) - h^{data}(t)| / h^{data}(t)}{T} \quad (9)$$

$$MAE = \frac{\sum_{t=1}^T |h^{sim}(t) - h^{data}(t)|}{T} \quad (10)$$

where $h^{sim}(t)$ is the simulated distance headway at time t , $h^{data}(t)$ is the actual distance headway from the field data at time t and T is the sample time.

Meanwhile, in order to facilitate the calibration of VIM, equation (6) can be rewritten as

$$a(t) = p \cdot \left[\frac{L_S}{D_d(t)^2} - \frac{L_S}{D(t)^2} \right] + q \cdot \frac{d}{dt} \left[\frac{L_S}{D(t)^2} \right] \quad (11)$$

where $p = m \cdot r^2$ and $q = n \cdot r^2$ denote the constant coefficients. Thus, the parameters to be

1 calibrated include p, q, t_d and s_0 . Besides, the vehicle back size L_S can be adjusted according
 2 to the leader's actual vehicle type.

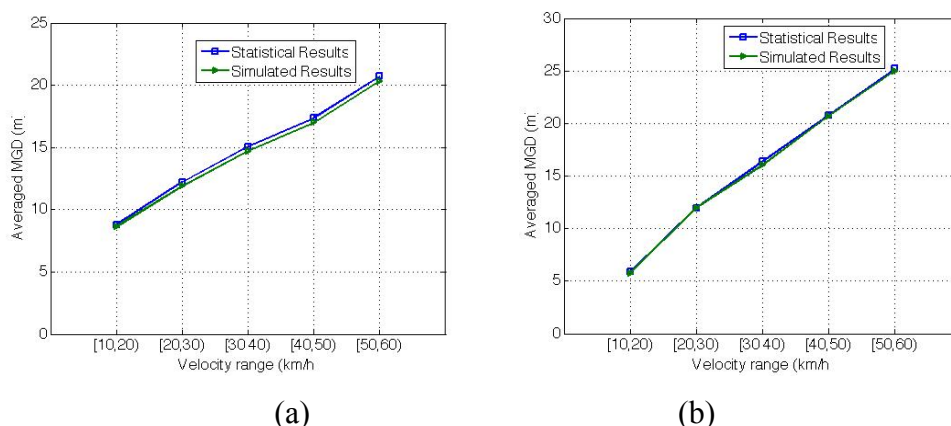
3
 4 **Single Trajectory Pair Based Evaluation**

5 The simulation processes are as follows. At the first step, model parameters of VIM are
 6 calibrated using Genetic Algorithm (GA) Toolbox in Matlab for each pair of leader-follower
 7 trajectories. At the second step, the calibrated model reproduces the trajectory of the
 8 following vehicle. Then at the third step, we calculate the MGD, MARE, and MAE. The
 9 three steps are repeated for each group of vehicle trajectories to obtain the Averaged MGD,
 10 Averaged MARE, Averaged MAE and Variance of MAE (VMAE)for C-C and C-T within
 11 different velocity ranges (cf. Table 2).
 12

13 **TABLE 2 Numerical Results by VIM Based on Field Data from US101**

	Velocity Range (km/h)	[10,20)	[20,30)	[30,40)	[40,50)	[50,60)
C-C	Averaged MGD (m)	8.6162	11.8826	14.7217	16.9896	20.3134
	Average MARE (%)	8.34%	7.83%	7.51%	6.83%	6.85%
	Averaged MAE (m)	0.3203	0.4545	0.5029	0.5515	0.6238
	VMAE	0.0888	0.2202	0.3342	0.3565	0.4292
C-T	Averaged MGD (m)	5.7544	11.9596	16.0330	20.7219	24.9656
	Average MARE (%)	3.45%	5.18%	4.69%	3.55%	1.46%
	Averaged MAE (m)	0.1253	0.3046	0.4209	0.3029	0.2924
	VMAE	0.0436	0.0960	0.2520	0.1479	0.3123

14 Note: for C-C the proper $L_S=1.8*1.6\text{ m}^2$; for C-T the proper $L_S=2.4*2.2\text{ m}^2$.



15
 16 **FIGURE 3 Comparison of averaged MGD in different velocity ranges.**
 17 **(a) C-C, (b) C-T.**
 18

19 In table 2, the simulated results show that the averaged MAREs are all smaller than 10%,

1 averaged MAEs do not exceed one meter and VMAEs are also within a small range, which
 2 illustrate the capability of VIM in reproducing the heterogeneous driving behaviors under
 3 different situations. Meanwhile, figure 3 demonstrates that under each group of vehicle
 4 trajectories, averaged MGDs simulated by VIM are consistent with the statistical results in
 5 table 1, which further verifies the performance of VIM in simulating the heterogeneous car
 6 following behaviors.

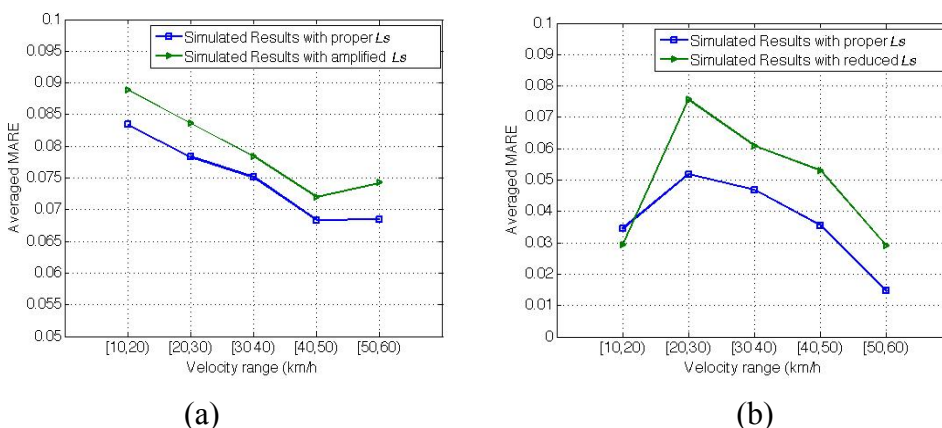
7 **Cross Comparison with Different L_S**

8 In VIM, L_S denotes the back size of the leading vehicle and is a parameter dependent on
 9 vehicle types. Therefore, VIM can directly capture the heterogeneous driving behaviors
 10 influenced by the leader’s vehicle type. In order to check the rationality of incorporating L_S
 11 into VIM, the trajectory reproducing tests are repeated with different L_S values. Table 3
 12 shows that although L_S is amplified or reduced, averaged MAREs are still below 10% and
 13 averaged MGDs are all close to simulation results in table 2. However, figure 4 illustrates that
 14 averaged MAREs produced by VIM with proper L_S are usually smaller than those by VIM
 15 with amplified or decreased L_S . This demonstrates the necessity of selecting appropriate L_S in
 16 VIM according to the leader’s actual vehicle type.

18 **TABLE 3 Cross Comparison Results by VIM Based on Field Data from US101**

	Velocity Range (km/h)	[10, 20)	[20, 30)	[30, 40)	[40, 50)	[50, 60)
C-C	Averaged MGD with amplified L_S (m)	8.6085	11.8181	14.5456	16.6529	19.7710
	Averaged MARE (%)	8.89%	8.36%	7.84%	7.20%	7.42%
C-T	Averaged MGD with reduced L_S (m)	5.9117	12.4262	16.7031	21.5760	25.7316
	Averaged MARE (%)	2.93%	7.56%	6.09%	5.30%	2.89%

19 Note: for C-C the amplified $L_S=1.9*1.8\text{ m}^2$; for C-T the reduced $L_S=1.8*1.6\text{ m}^2$.



20
 21
 22 **FIGURE 4 Comparison of MAREs in various velocity ranges. (a) C-C, (b) C-T.**

1 Vehicle Type Based Evaluation

2 In order to evaluate the performance of VIM, two well-known car-following models based on
 3 3-D traffic information (i.e. Optimal Velocity Model (OVM) and Intelligent Driver Model
 4 (IDM)) and one model utilizing visual angle information (i.e. Driving by Visual Angle Model
 5 (DVA)) are used as the reference models for comparison (See **Appendix A**). Different from
 6 single trajectory pair based evaluation where model parameters are calibrated for each pair of
 7 car-following trajectories, in the vehicle type based evaluation, only one set of parameters is
 8 calibrated for C-C and C-T respectively. The detailed processes can be described as follows.

9 Firstly, any pair of leader-follower trajectories that lasts for about 30 seconds should be
 10 selected from US101 data and distributed into the corresponding group based on its
 11 leader-follower composition, e.g. C-C or C-T; At the second step, with regard to each group
 12 of leader-follower trajectories, one set of model parameters are calibrated respectively for
 13 VIM、OVM、IDM and DVA by Genetic Algorithm (GA) Toolbox in Matlab; Thirdly, these
 14 four calibrated models are validated by the other different group of leader-follower
 15 trajectories, which can also be called cross-validation; Finally, the calibration and validation
 16 results both denoted by MAREs can be utilized to compare the predicting performance of
 17 these four models.

18

19 **TABLE 4 Calibration and Validation Results by Different Models**

	VIM		OVM		IDM		DVA	
Calibration (C-C data)	MARE	20.95%	MARE	22%	MARE	35.28%	MARE	63.28%
	t_d [s]	1.3534	α [s^{-1}]	1.0587	v_0 [m/s]	35.788	t_d [s]	0.3627
	p [1]	342.61	V_1 [m/s]	1.6648	s_0 [m]	3.8538	j [1]	2.1762
	q [1]	-29.423	V_2 [m/s]	12.86	T [s]	0.2273	k [1]	-0.1011
	s_0 [m]	4.4985	C_1 [m^{-1}]	0.2187	a [m/s^2]	9.1451		
			C_2 [1]	1.7382	b [m/s^2]	0.3890		
					δ [1]	16.114		
Validation (C-T data)	MARE	13.93%	MARE	14.28%	MARE	23.84%	MARE	45.69%
Calibration (C-T data)	MARE	13.97%	MARE	14%	MARE	22.76%	MARE	41.29%
	t_d [s]	1.4980	α [s^{-1}]	0.6460	v_0 [m/s]	93.635	t_d [s]	0.5737
	p [1]	339.59	V_1 [m/s]	4.9176	s_0 [m]	2.0259	j [1]	0.2482
	q [1]	-1.1157	V_2 [m/s]	10.151	T [s]	0.0424	k [1]	-3.6040
	s_0 [m]	3.5065	C_1 [m^{-1}]	0.2955	a [m/s^2]	7.1418		
			C_2 [1]	2.9622	b [m/s^2]	0.2158		
					δ [1]	12.469		

Validation (C-C data)	MARE	22.51%	MARE	22.71%	MARE	38.17%	MARE	55.88%
--------------------------	------	--------	------	--------	------	--------	------	--------

Note: the number of the pair of leader-follower trajectories for C-C is 2556 and that for C-T is 154.

Results in table 4 show that MAREs generated by VIM during the processes of calibration and validation are smaller than those obtained by other three reference models, which not only implies the better predictive performance of VIM in calibration process but also illustrates the better adaptability of VIM in validating the heterogeneous driving behaviors through adjusting the parameter about the back size of the leading vehicle.

Moreover, the performance of these four models can also be further evaluated by inspecting one individual pair of leader-follower trajectories. As for C-C, MAREs in calibration process are 5.63%, 8.70%, 9.09% and 6.58% respectively for VIM, OVM, IDM and DVA, and as for C-T, these values are 6.10%, 7.04%, 6.77% and 13.39% respectively (See figure 5 for visual demonstration). Obviously, when comprehensively comparing these calibration results at the level of single trajectory pair it is easily known that the predicting performance of VIM is more superior than that of other three reference models.

Therefore, above evaluation results at the levels of vehicle type and single trajectory pair show the superiority of VIM in reproducing the trajectory of the following vehicle to other three models for both C-C and C-T. In summary, VIM can better describe the heterogeneous driving behaviors influenced by the leader's vehicle type.

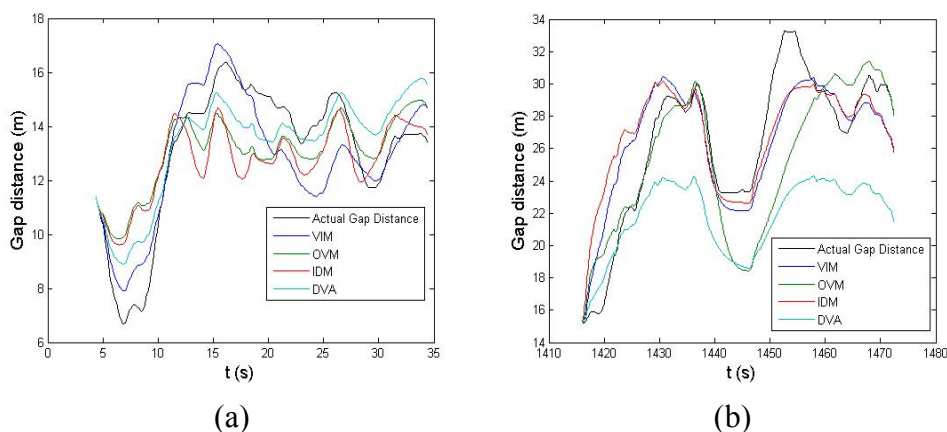


**FIGURE 5 Gap distance fluctuation reproduced by different models.
(a) C-C, (b) C-T.**

1 CONCLUSIONS

2 This paper proposes a visual imaging model (VIM) to describe the heterogeneous
3 car-following dynamics among different vehicle types. Most traditional car following models
4 (e.g. OVM and IDM) assumed that drivers are perfectly rational and can perceive the 3-D
5 traffic information accurately. On the other hand, those models also do not include parameters
6 that are dependent on vehicle types, which is a critical to model the heterogeneous driving
7 behaviors. Existing visual angle based models only utilizes the 2-D visual angle extent of the
8 leading vehicle or its changing rate as the visual stimulation, which can not describe the
9 whole visual stimulus subtended by the preceding vehicle. The proposed VIM can overcome
10 those shortcomings with the visual imaging size of the leading vehicle and its change rate
11 treated as the stimuli to the follower. Moreover, VIM is also suitable for describing the
12 heterogeneous driving behaviors by adjusting the parameters L_S according to the leader's
13 vehicle type. The model also ensures that under the small gap distance, the larger back size of
14 the leading vehicle can cause stronger stimulus to the follower that result in the greater
15 acceleration or deceleration, but when the gap distance is relatively large, the follower is not
16 sensitive to the back size of the preceding vehicle, which is consistent with the empirical
17 driving experience.

18 The model is further evaluated by conducting calibration at the level of single trajectory
19 pair and implementing the calibration and validation at the vehicle type level. At the level of
20 single trajectory pair, calibrated VIM is able to reproduce the results of averaged MGDs
21 found in statistical analysis about the US101 NGSIM data, which is that the average MGD
22 for C-C is larger than that for C-T at low velocity range but smaller than that for C-T at high
23 velocity range. At the level of vehicle type, the calibration and validation results by the model
24 are compared with those by other three reference models and favorable conclusions for the
25 model are obtained, which show that the calibrated VIM has more predicting performance in
26 car following dynamics than those three reference models under heterogeneous
27 leader-follower compositions (i.e. C-C and C-T) because of the vehicle type related
28 parameter incorporated in the proposed VIM.

29 Further research about other kinds of heterogeneity in car following behaviors will be
30 conducted with VIM from the field data, such as various driving styles related to their own
31 different vehicle types and different driving styles within the group of the same vehicle type.
32 Meanwhile, the proposed model has the potential to be extended to more comprehensive and

1 realistic 3-D microscopic simulation models to account for full information on the road (e.g.
 2 the 3-D size and shape of the surrounding vehicles, road side objects, curvatures) that can
 3 affect microscopic driver behavior.

5 ACKNOWLEDGEMENTS

6 This paper was partly supported by National Natural Science Foundation of China (Grant No.
 7 70971094), National Natural Science Youth Foundation of China (Grant No. 50908155),
 8 Program for Changjiang Scholars and Innovative Research Team in University (PCSIRT).

10 APPENDIX A

11 Optimal Velocity Model (OVM)

12 Optimal Velocity Model (OVM) was firstly proposed by Bando et al.(12) and formulated as

$$13 \quad a_n(t) = \alpha \{V[\Delta x_n(t)] - v_n(t)\}$$

14 where $a_n(t)$ is the acceleration of vehicle n at time t , $V[\Delta x_n(t)]$ is the optimal velocity
 15 depending on the distance headway, $\Delta x_n(t)$ and $v_n(t)$ are respectively the distance headway
 16 and velocity of vehicle n at time t , α is the sensitivity coefficient. Besides, the selected OV
 17 function is written as $V[\Delta x_n(t)] = V_1 + V_2 \tanh\{C_1[\Delta x_n(t) - l_n] - C_2\}$, where l_n is the length of
 18 vehicle n , V_1, V_2, C_1 and C_2 are four main parameters in the OV function (29).

20 Intelligent Driver Model (IDM)

21 Treiber et al. (30) proposed Intelligent Driver Model (IDM) and defined it by the following
 22 acceleration function

$$23 \quad a_{IDM} = a \left\{ 1 - \left(\frac{v}{v_0} \right)^\delta - \left[\frac{s^*(v, \Delta v)}{s} \right]^2 \right\}, \text{ where } s^*(v, \Delta v) = s_0 + T \cdot v + \frac{v \cdot \Delta v}{2\sqrt{ab}}.$$

24 where v_0 is the desired velocity, v is the current velocity, a is the maximum acceleration, δ
 25 is the acceleration component, s is the current gap distance, s_0 is the minimum distance in
 26 congested traffic, T is the safe time gap for following the leading vehicle, b is the maximum
 27 desired deceleration and Δv is the velocity difference between the leader and the follower.

29 Visual Angle Model (DVA)

1 Andersen et al.(18) presented Driving by Visual Angle Model (DVA) to replace the
2 3-Dinformation with the optical information, which is formulated as

$$3 \quad a_{DVA} = j \cdot \left(\frac{1}{\alpha} - \frac{1}{\alpha^*} \right) + k \cdot \frac{d}{dt} \alpha$$

4 where $j > 0$ and $k < 0$ are constants, α and α^* are respectively the current and desired visual
5 angle extent of the leading vehicle, $d\alpha/dt$ is the change rate of α . Moreover, α and α^* can be
6 expressed as

$$7 \quad \alpha = \frac{w}{D(t)} \text{ and } \alpha^* = 2 \cdot a \tan\left(\frac{w}{t_d \cdot v_f}\right).$$

8

9 REFERENCE

- 10 (1) Ossen, S., and S.P. Hoogendoorn. Heterogeneity in car-following behavior: Theory and
11 empirics. *Transportation Research Part C*. Vol. 19, 2011, pp. 182-195.
- 12 (2) Ossen, S., and S.P. Hoogendoorn. Driver Heterogeneity in car following and its impact on
13 modeling traffic dynamics. *Transportation Research Record*. No. 1999, 2007, pp: 95-103.
- 14 (3) Ranjitkar, P., T. Nakatsuji, and M. Asano. Calibration and validation of microscopic traffic
15 flow models using PTK GPS data. *Proc. of the Int. Conf. on Application of Advanced*
16 *Technologies in Transportation Engineering*. ASCE, Reston, VA, Vol. 144, 2004a, pp:
17 395-400.
- 18 (4) Punzo, V., and A. Tripodi. Steady-state solutions and multiclass calibration of gipps
19 microscopic traffic flow model. *Transportation Research Record*. No. 1999, 2007, pp:
20 104-114.
- 21 (5) Parker, M. T.. The effect of heavy goods vehicles and following behavior on capacity at
22 motorway road work sites. *Traffic Engineering and Control*. Vol. 37, Issue 9, 1996, pp:
23 524-531.
- 24 (6) Sayer, J. R., M.L. Mefford, and R. Huang. The effect of lead vehicle size on driver
25 following behavior: Is ignorance truly bliss? In: *Proceedings of the 2nd international driving*
26 *symposium on human factors in driver assessment, Training and Vehicle Design*, University
27 of Iowa, 2003.
- 28 (7) Brackstone, M., B. Waterson, and M. McDonald. Determinants of following distance in
29 congested traffic. *Transportation Research Part F*. Vol. 12, Issue 2, 2009, pp: 131-142.
- 30 (8) Yoo, H., and P. Green. Driver behavior while following cars, trucks and buses, Report no.

- 1 UMTRI-99-14. Ann Arbor, MI: The University of Michigan Transportation Research Institute,
2 1999.
- 3 (9) Ravishankar, K.V. R., and Tom V. Mathew. Vehicle-type dependent car following model
4 for heterogeneous traffic conditions. *Journal of transportation engineering*. Vol. 137, No. 11,
5 2011, pp: 775-781.
- 6 (10) Chandler, R.E., R. Herman, and E.W. Montroll. Traffic dynamics: Studies in car
7 following. *Operation Research*. Vol. 6,1958, pp: 165-184.
- 8 (11) Gipps, P.G..A behavioural car-following model for computer simulation. *Transportation*
9 *Research Part B*. Vol. 15, Issue 2, 1981, pp: 105-111.
- 10 (12) Bando, M., K. Hasebe, A. Nakayama, A. Shibata, and Y. Sugiyama. Dynamical model of
11 traffic congestion and numerical simulation. *Physical Review E*. Vol. 51, 1995, pp:
12 1035-1042.
- 13 (13) Lee, D. N.. A theory of visual control of braking based on information about time to
14 collision. *Perception*. Vol. 5, 1976, pp: 437-459.
- 15 (14) Evans, L., and R. Rothery. Perceptual thresholds in car following-a recent comparison.
16 *Transportation Science*. Vol. 11, 1977, pp: 60-72.
- 17 (15) Brackstone, M., and M.McDonald. Car-following: A historical review. *Transportation*
18 *Research Record F*. Vol. 2, 1999, pp: 181-196.
- 19 (16) Brackstone,M., B.Sultan, and M.McDonald. Motorway driver behavior: Studies in car
20 following. *Transportation Research Record F*. Vol. 5, 2002, pp: 31-46.
- 21 (17) Ferrari, P..The effect of driver behavior on motorway reliability. *Transportation Research*
22 *Part B*. Vol. 23B, Issue 2, 1989, pp: 139-150.
- 23 (18) Andersen, G.J., and C.W. Sauer. Optical information for car following: The driving by
24 visual angle model. *Human Factors*. Vol. 49, 2007, pp: 878-896.
- 25 (19) Helly, W.. Simulation of bottlenecks in single lane traffic flow. In *Proceedings of the*
26 *Symposium on the Theory of Traffic Flow*, Elsevier, New York, NY, 1959, p: 207-238.
- 27 (20) Jin, S., D.H. Wang, Z.Y. Huang, and P.F. Tao. Visual angle model for car following
28 theory. *Physica A*. Vol. 390, 2011, pp: 1931-1940.
- 29 (21) Lee, J., and J.H. Jones. Traffic dynamics: Visual angle car following models. *Traffic*
30 *Engineering and Control*, Vol. 8, 1967, pp: 348-350.
- 31 (22) Lee, D.N.. A theory of visual control of braking based on information about time to

- 1 collision. Perception. Vol. 5, 1976, pp: 437-459.
- 2 (23) Hoffman, E.R., and R.G. Mortimer. Driver's estimates of time to collision. Accident
- 3 Analysis and prevention. Vol. 26, 1994, pp: 511-520.
- 4 (24) Sidaway,B., M.Fairweather, H. Sekiya, and J. McNitt-Gray. Time-to-collision estimation
- 5 in a simulated driving task. Human Factors. Vol. 38, 1996,pp: 101-113.
- 6 (25) Michaels,R. M.. Perception factors in car following. In Proceedings of the Second
- 7 International Symposium on the Theory of Road Traffic Flow, OECD, Paris, 1963, p:44-59.
- 8 (26) Zielke, T., M. Brauckmann, and W. von Seelen. Intensity and edge based symmetry
- 9 detection with an application to car following. Computer Vision, Graphics, and Image
- 10 Processing. Vol. 58, 1993, pp: 177-190.
- 11 (27) NGSIM. Next Generation Simulation.ngsim.fhwa.dot.gov, 2006.
- 12 (28) Bennett,C.R..A speed prediction model for rural two-lane highways, PhD thesis, The
- 13 University of Auckland, New Zealand, 1994.
- 14 (29) Helbing, D., and B. Tilch. Generalized force model of traffic dynamics. Physical Review
- 15 E. Vol. 58, Issue 1, 1998, pp: 133-138.
- 16 (30) Treiber, M., A. Hennecke, and D. Helbing. Congested traffic states in empirical
- 17 observations and microscopic simulations. Physical Review E. Vol. 62, 2000, pp: 1805-1824.